APPLICATION OF CNN ON LANDSLIDE SUSCEPTIBILITY ANALYSIS: CASE STUDY ON 2018 HOKKAIDO EASTERN IBURI EARTHQUAKE

Karl Malcolm N. Cordova[1,2], Tanakorn Sritarapipat[1,3*], Pantip Piyatadsananon[1,4]
[1]School of Geoinformatics, Suranaree University of Technology, Nakhon Ratchasima 30000 Thailand,
[2]Email: karl.cordova81@gmail.com
[3*]Email: tanakorn.s@sut.ac.th
[4]Lower Northeast Regional Center of Geoinformatics and Space Development Agency (SUT), Suranaree University of Technology, Nakhon Ratchasima 30000 Thailand
Email: pantip.p@sut.ac.th

KEY WORDS: landslides, deep learning, convolutional neural network

ABSTRACT: Landslides are one of the most common geohazards occurring worldwide. Landslide susceptibility mapping is crucial to vulnerable areas in terms of mitigating the future impacts from this reoccurrence. Landslide susceptibility mapping has been generated for a long time with standard methods such as fuzzy logic, analytical hierarchy process (AHP), and logistic regression. Recently, conventional machine learning algorithms have been considered as an advanced technique for landslide susceptibility mapping. In addition, it is possible to use artificial neural networks and deep learning models in place of conventional machine learning algorithms to provide significant results. This study proposes a deep 1-dimensional convolutional neural network (CNN-1D) model to predict landslides and evaluate its performance on landslide susceptibility mapping. The proposed model was applied to Hokkaido prefecture, where 4,350 landslide scars have been extracted and identified from satellite images dated shortly after the 2018 Hokkaido Eastern Iburi earthquake. As a result, the CNN-1D model provides 96% accuracy, with 97% precision on the landslide class with 94% recall. In conclusion, applying the deep learning technique (CNN-1D model) can yield a significantly accurate landslide susceptibility map.

1. INTRODUCTION

Japan Meteorological Agency (JMA) recorded a 6.6-moment magnitude earthquake at the coast of Tomakomai City in the eastern Iburi subprefecture on September 9th, 2018. Tremors were felt strongly in the neighboring Aomori Prefecture in the Tohoku region, with minor shocks experienced in the Kanto region. The earthquake caused subsequent landslides to occur in the neighboring town of Atsuma, where the volcanic soil already saturated by Typhoon Jebi triggered slope failures leaving dozens of homes and leaving several residents dead. Zhang et al. (2019) further concluded that slope failures occurred in stratified pyroclastic fall deposits overlaying Miocene sedimentary bedrock, with sliding liquefaction observed on field investigations. In the subsequent aftermath, an estimated 367.5 billion yen in damages was reported in Hokkaido. The 2.95 million households were left without electricity due to damages to the Hokuden coal power plant in Atsuma. In order to mitigate the socio-economic impact of future landslides and identify risk areas, landslide susceptibility mapping should be conducted. In conducting such studies on disaster risk, however, choosing an accurate model becomes necessary. In the past years following the 2018 Eastern Iburi earthquake, several researchers have used different machine learning algorithms and neural networks for landslide susceptibility mapping in the areas affected by the disaster. Nam and Wang (2019) previously investigated the use of autoencoders to analyze patterns similar to the landslide scarps identified in the steep mountainous areas to obtain an accuracy of 91.1% for the best model. In the same year, Aimati et al. (2019) also conducted a study of the same area in the town of Atsuma by applying a tree-based model in identifying landslide locations on SAR images, getting an overall accuracy of 80.1%. Liu et al. (2021) introduced a novel method of applying a hybrid ensemble model that integrated a Geo-detector (spatial stratified heterogeneity) tool into a random forest model. The hybrid model recorded consistent accuracy on all datasets, with the highest being 89.09%. A more recent study by Nava et al. (2021) investigated how deep learning CNN can be used to improve landslide detection on Sentinel-2 and SAR datasets, with the highest accuracy recorded at 94.17%. This research aims to use a one-dimensional convolutional neural network (CNN-1D) to create a landslide susceptibility map of southern Hokkaido Prefecture. This study also investigated the predictive performance of CNN-1D in identifying landslide-risk areas based on data visually analyzed and extracted from previous satellite images of the study area.

2. METHODOLOGY

2.1 Study Area

The study focused on a portion of Hokkaido covering a total of 10 towns and cities on three subprefectures: Iburi (Abira, Atsuma, Mukawa, Tomakomai City), Ishikari (Chitose City, Eniwa City), Sorachi (Kuriyama, Naganuma, Yubari City, Yuni). The area is a lowland of Late Pleistocene fluvial deposits and pyroclastic volcanic rocks in the west. Detrital sedimentary rocks underlie the hilly central area. The rugged terrain in the east is a complex lithologic landscape due to the presence of fluvial, marine, and detrital sedimentary rocks alongside alternating beds of sedimentary and ash deposits. Mafic plutonic rocks found in the area indicate probable tectonic movement (Zhang et al., 2018).

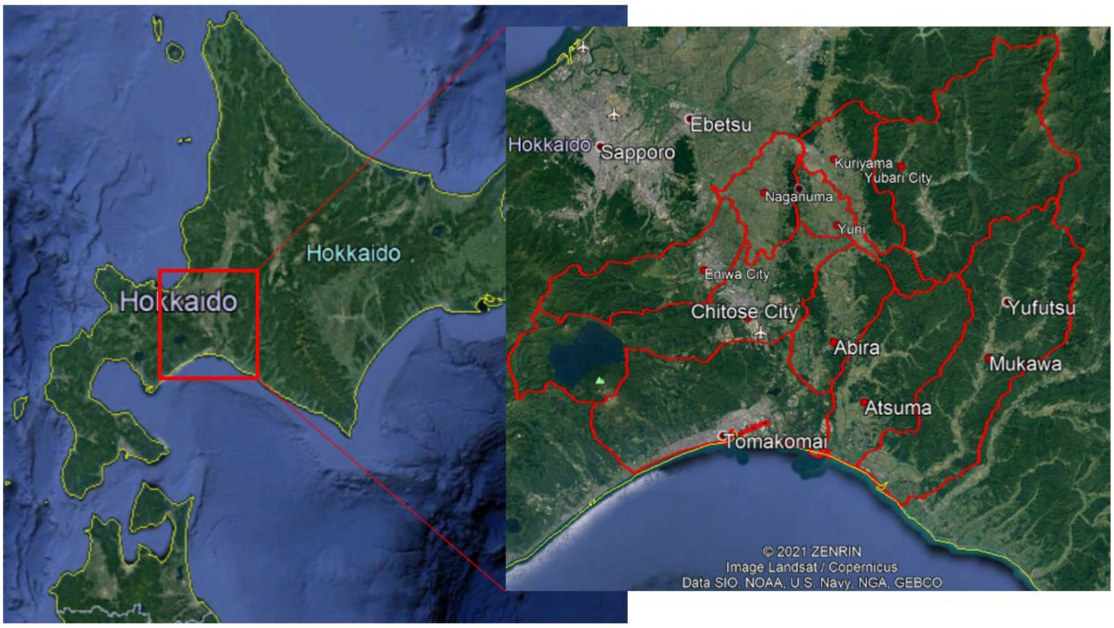

Figure 1. Google Earth image of the study area showing the town and city boundaries.

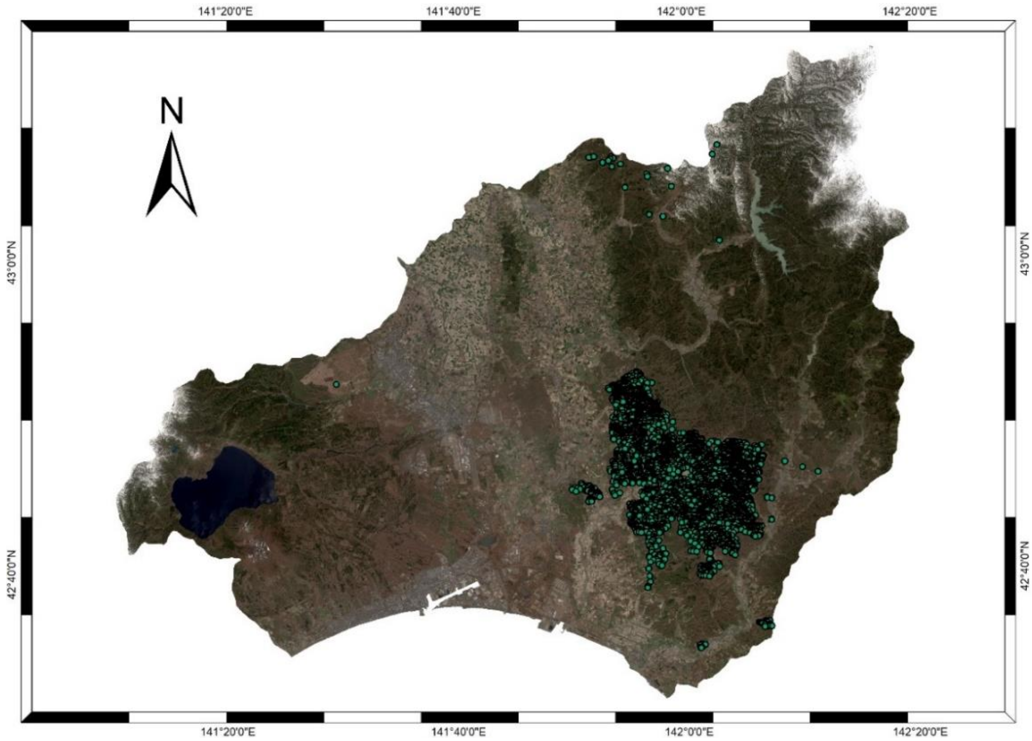

. Figure 2. 10m satellite image of the study area dated May 7th, 2021, showing landslide points (modified from Copernicus Sentinel data [2021])

2.2 Data Acquisition

A 10m resolution satellite image of Hokkaido from Sentinel-2A satellite dated October 20th, 2018, was used to identify landslide scarps. Landslide scarps were visually analyzed and extracted, with a total of 4350 points identified. A recent satellite image from Sentinel-2A dated May 7th, 2021, was used for extracting the NDVI of the study area. For binary classification tasks, an equal number of non-landslide points were randomly generated on locations deemed a low risk to landslides based on their topography. The weather data encompasses the twenty-year annual precipitation of Hokkaido prefecture based on 22 stations. The weather data is interpolated using the Inverse Distance Weighting function with the resulting geostatistical layer resampled into a 10m raster. The geologic map is manually digitized, with each stratigraphic group clustered together according to predominant rock units reducing the number of units to six. Unique geologic units were separated and converted into binary dummy variables.

Table 1 Data resources of the study

Data	Data type	Source
10 m multispectral image	Raster (satellite image)	Sentinel-2A (EarthExplorer)
10 m DEM	Raster mesh grid (JPGIS/XML)	Geospatial Information Authority of Japan (https://fgd.gsi.go.jp/download/menu.php)
Geologic map (1:200,000)	Raster (GeoTIFF)	Geological Survey of Japan (https://www.gsj.jp/Map/index_e.html)
Weather Data	Table	Japan Meteorological Agency (JMA) https://www.data.jma.go.jp/obd/stats/data/en/smp/index.html
Fault map	Shapefile (polyline)	GEM Global Active Fault Database (https://github.com/GEMScienceTools/gem-global-active-faults)

2.3 Selection of Landslide Parameters

Landslide parameters were selected based on their influences in inducing downslope soil movement. In general, slopes with a higher degree of the gradient are more susceptible to landslides. Differences in slope aspect affect the degree of precipitation and solar radiation, while curvature reflects terrain complexity and topography (Zhang et al., 2019). Soil and lithology effectively influence landslides due to differences in shear strength, porosity, density, and particle sizes. Seismic energy released by faults can effectively trigger landslides in steep areas with weak soil foundations. Hydrological factors such as TWI, rainfall, and stream flow influence soil movements as sediments are suspended and can travel the same direction as water. Additionally, moisture can also affect soil cohesion through saturation. The amount and condition of vegetation are reflected in the NDVI. Areas with higher vegetation are generally at lower risk of landslides as root cohesion effectively strengthens the underlying soil and prevents it from being carried and transported by erosional agents. Sixteen-landslide parameters were used in the study, including six unique geologic units that were converted into dummy variables. Values of each landslide parameter are extracted into landslide and non-landslide points for binary classification tasks and exported as a CSV file. Prior to feeding as input into the CNN-1D model, each landslide parameter was preprocessed using the Minimum and Maximum Scaling, which scales the value of each feature into a range between 0 and 1. The input data was split into 70% training and 30% validation.

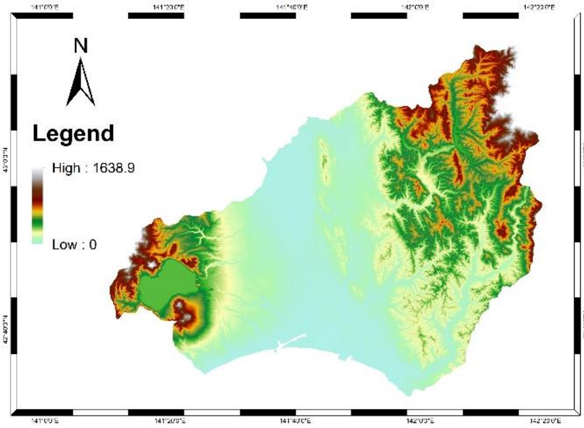

Figure 3. Elevation (meters)

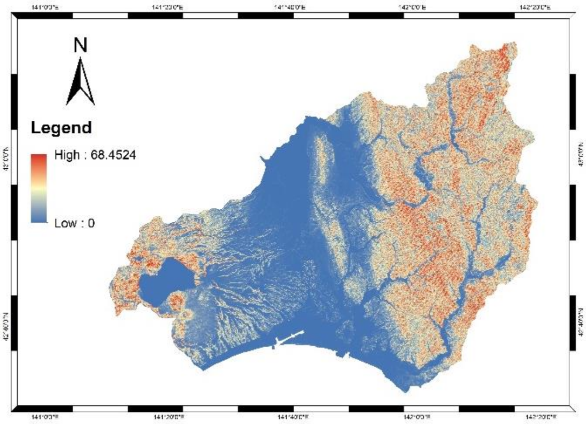

Figure 4. Slope (degrees)

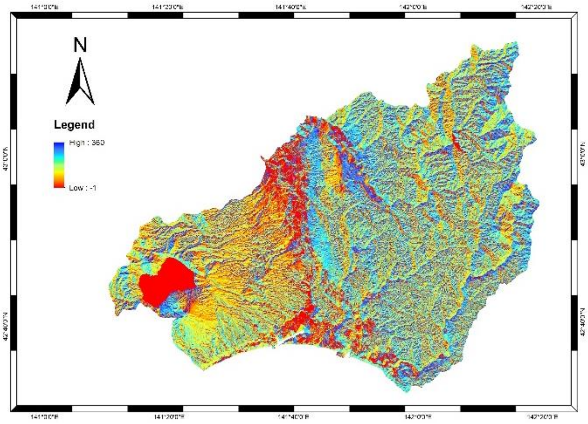

Figure 5. Aspect

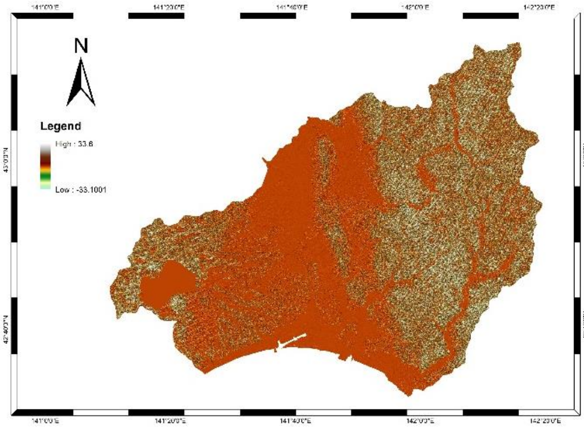

Figure 6. Curvature

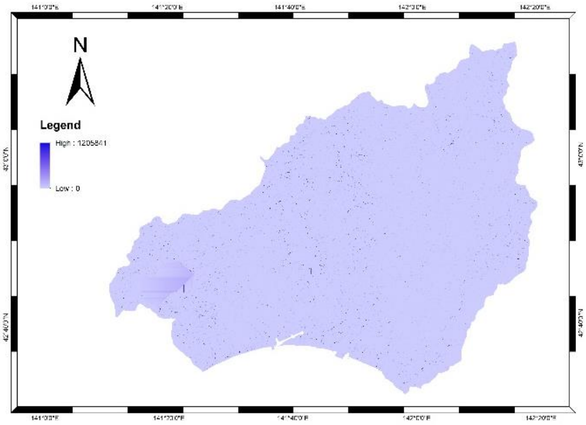

Figure 7. Flow accumulation

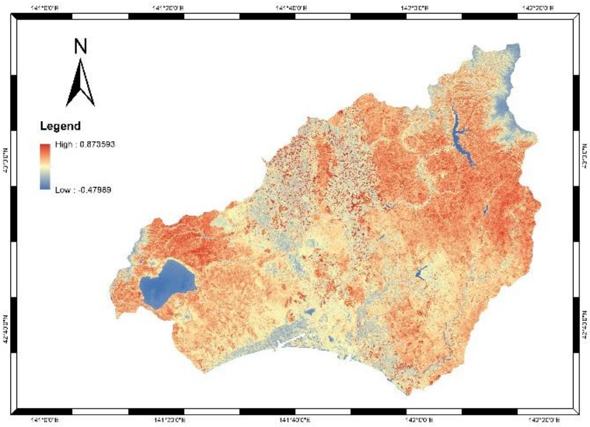

Figure 8. NDVI

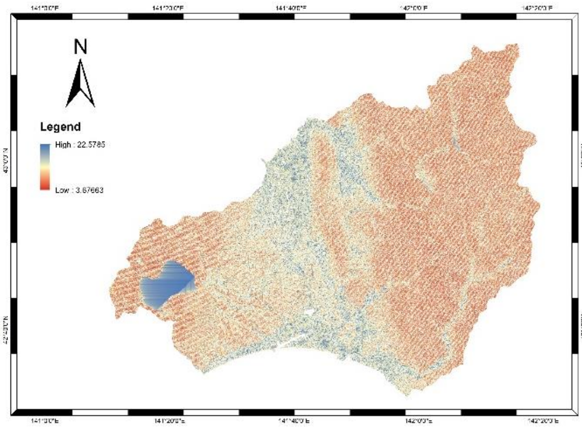

Figure 9. TWI

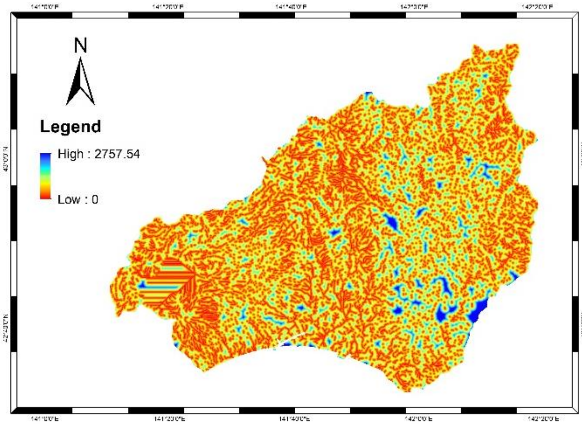

Figure 10. Distance to stream (meters)

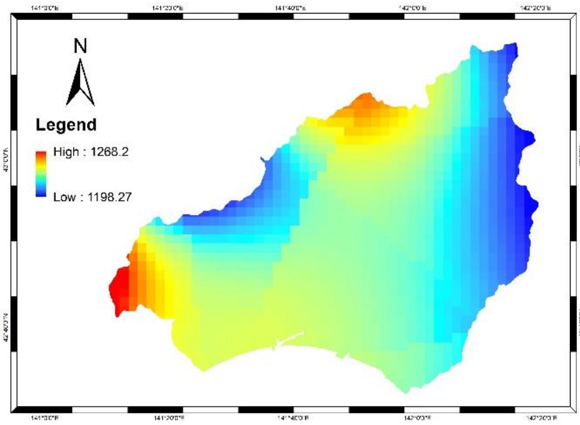

Figure 11. Mean annual precipitation (mm.)

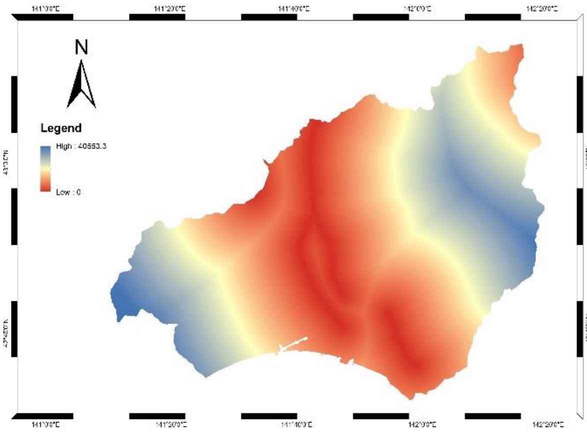

Figure 12. Distance to fault line (meters)

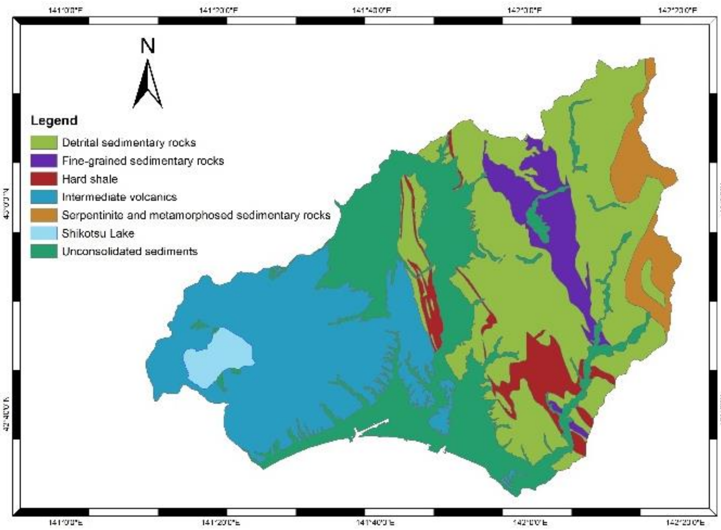

Figure 13. Geologic units

2.4 CNN-1D Architecture

Similar to its 2D and 3D counterparts, it consists of a convolutional layer that filters input data with *N* kernels connected to a pooling layer that subsamples the preceding layer's resulting output (Wang et al., 2019). Whereas CNN-1D was typically used for predicting temporal data, such as in the case of signal processing (Abdeljaber et al., 2017) and wind prediction (Harbola and Coors, 2019), the method was applied on landslide susceptibility mapping with high predictive accuracy, such as in the works of Wang, et al. (2019) and Fang, et al. (2020). The main difference between CNN-1D and its traditional 2D counterpart is that it works by convolving input data into a 1d array instead of a 2d matrix (Abdeljaber et al., 2017). A 1D convolutional filter takes on 3d tensor data with input shape equal to the batch shape (None for an arbitrary number of samples), many steps, and input dimension. For geospatial analysis using the CSV file as input data, the number of steps signifies the number of bands or independent variables, with the input dimension being 1.

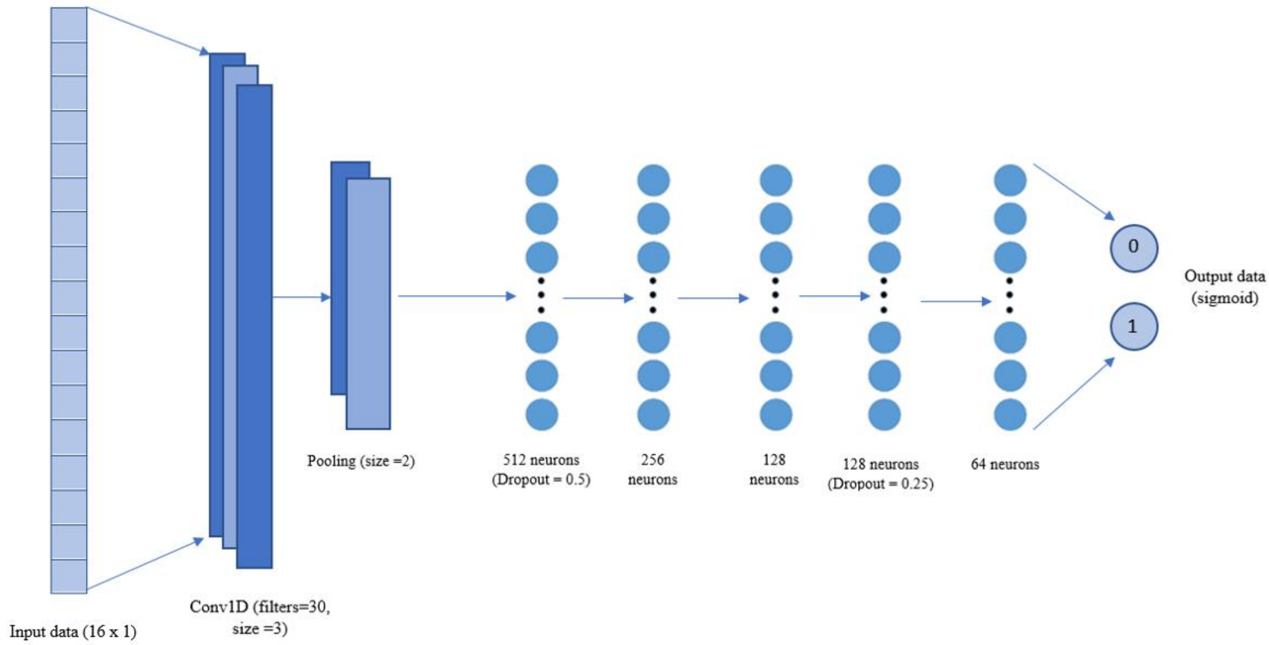

Figure 14. The Architecture of the proposed CNN-1D model

The CNN architecture used in this study comprises a single 1D convolutional layer with 30 filters and a kernel size of 3 with a ReLU (rectified linear unit) activation function. The output of the filter is fed to a max-pooling layer with a pool of 2 and flattened prior to input into a standard multilayer perceptron (MLP) classifier. The first hidden layer of the MLP is composed of 512 neurons with a dropout of 0.5. The second layer consisted of 256 neurons. The third and fourth layers comprised 128 neurons, with the latter having a dropout of 0.25. The fifth hidden layer was composed of 64 neurons connected to the output layer with two nodes. All hidden layers have the ReLU activation function except the output layer, which uses the sigmoid function for binary classification tasks. The architecture is optimized using the stochastic gradient descent method Adam with a learning rate of 0.0003. The model was modified from Fang et al. (2020).

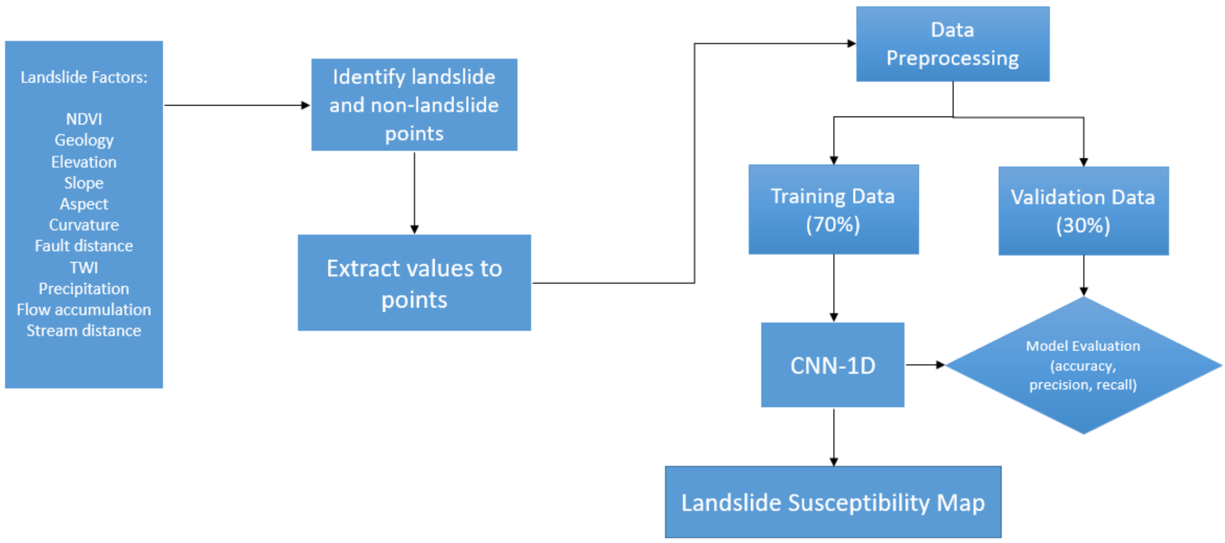

Figure 15. Flowchart of the methodology

3. RESULTS AND DISCUSSION

3.1 Model Results

Prior to training, the compiled model is fitted with an early-stopping callback which stops the training routine when validation loss increases after five iterations. The compiled model was modified to create a separate model without early-stopping callbacks with 100 epochs. The first model converged after 22 epochs with a final training accuracy and validation accuracy of 89.99% and 91.3%, respectively. The second model without early-stopping callbacks showed greater performance improvement, leading to a training accuracy of 94.8% with validation accuracy of 95.8%. Evaluation metrics showed that the second CNN-1D model accurately classified 97% of landslide points with a recall (sensitivity) of 94% and F1-score of 96%. In classifying non-landslide classes, the model showed a precision of 94%, while the recall value (specificity) for this class is higher at 97%, with an F1-score of 96%.

Table 2. Classification report of the CNN-1D model

	Precision	Recall	F-1 score
Non-landslide	94%	97%	96%
Landslide	97%	94%	96%
Accuracy			96%

Further tests were also conducted by increasing the number of epochs beyond 100. However, the tests showed diminishing returns in accuracy and were also observed to directly affect the final output image, resulting in darker images that lack any factual information.

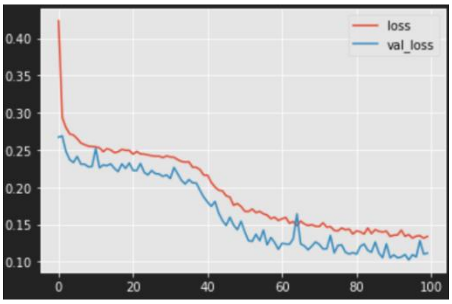

Figure 16. Model loss plot

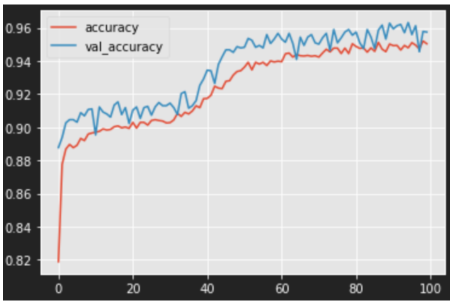

Figure 17. Accuracy loss plot

3.2 Landslide Susceptibility Map

Due to hardware constraints, all input data are divided into three separate datasets representing the subprefectures. This is to reduce prediction time and avoid any memory-related issues that come with handling extensive datasets. The three predicted landslide susceptibility maps are classified using geometric intervals and designated with five discrete classes ranging from very low to very high to represent susceptibility levels. The choice of using geometric intervals is that the three maps are initially part of one large dataset. Geometric interval minimizes the sum of squares of elements in each class. The consistent values in the intervals defined by the natural breaks came from specific data classification, which could not be compared with multiple maps.

A total area of 4070.81 sq. km. was mapped, covering several portions of 3 subprefectures. As a result, 552.88 sq. km. (43.59% of the total area) were classified as very high susceptibility to landslides. In contrast, 461.63 sq. km (36.39% of the area) were classified as very low susceptibility in Sorachi subprefecture. In the Iburi subprefecture, where most of the landslides were identified, 816.63 sq. km. or 42.66% of the mapped areas, as very high susceptibility to landslides. Areas with very low vulnerability were slightly higher at 770.25 sq. km. or 40.24% of the total mapped area of the subprefecture. In the mapped areas of Ishikari subprefecture, 369.27 sq. km. or 41.58% of the total area mapped was classified as very low susceptibility. Almost half of the area was classified as very high susceptibility for 431.04 sq. km. or 48.53% of the study area. For the study area, 39.33% were classified as very low susceptibility, while 44.23% were classified as very high susceptibility. The summary of landslide susceptibility classes across three subprefectures shows in Table 3.

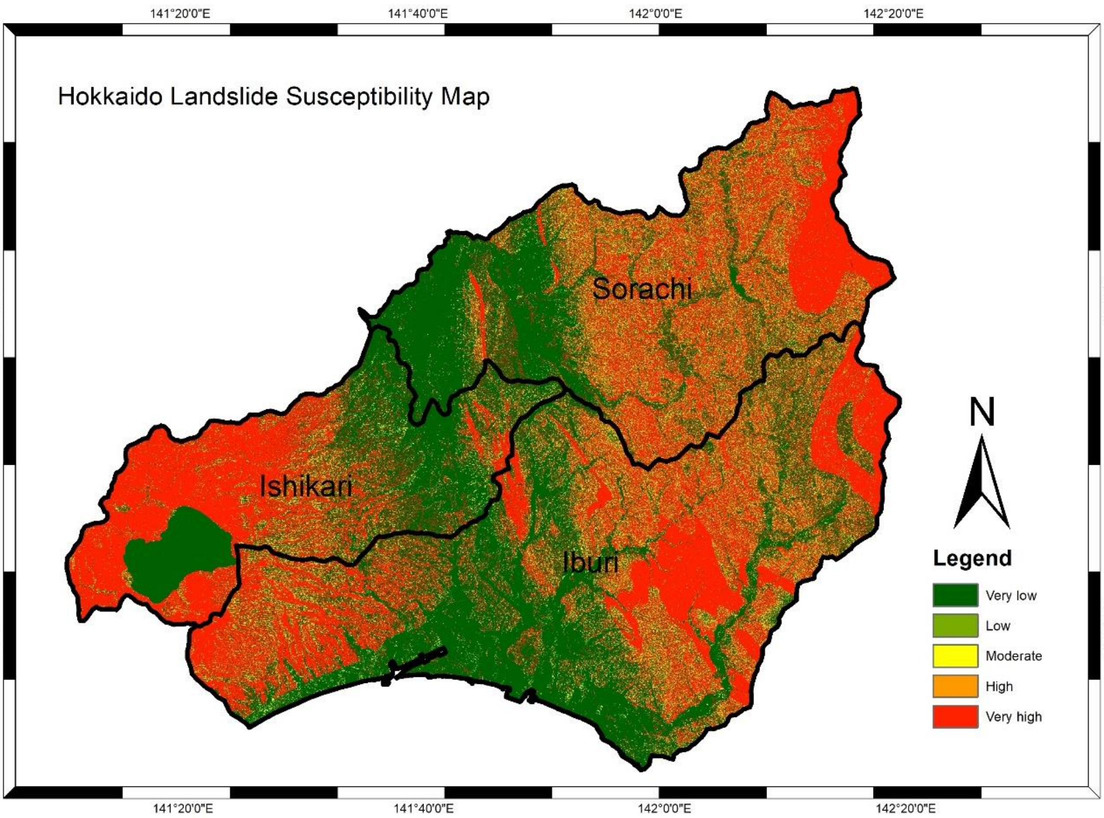

Figure 18. Landslide susceptibility map of the study area showing subprefecture boundaries

Table 3. Areas of landslide susceptibility in each subprefecture

Susceptibility	Sorachi (sq. km.)	Area percent	Iburi (sq. km.)	Area percent	Ishikari (sq. km.)	Area percent
Very low	461.63	36.39	770.25	40.24	369.27	41.58
Low	82.8	6.53	99.11	5.18	20.28	2.28
Moderate	128.88	10.16	168.64	8.81	47.6	5.36
High	42.21	3.33	59.6	3.11	20.01	2.25
Very high	552.88	43.59	816.63	42.66	431.04	48.53
Total	1268.39		1914.22		888.2	

Table 4. Landslide susceptibility classes of the entire study area

Susceptibility	Area (sq. km.)	Area percent
Very low	1601.15	39.33
Low	202.19	4.97
Moderate	345.12	8.48
High	121.81	2.99
Very high	1800.55	44.23
Total	4070.81	

3.4 Comparison with Logistic Regression model

For benchmark purposes, a separate test was conducted using the standard logistic regression model. The standard logistic regression model showed similar results with the CNN-1D model with an overall accuracy of 96% while decreasing precision in classifying landslide points. However, it should be noted that no further tests were conducted, such as ANOVA, AIC, or R-squared statistics, to measure the validity of this model. The comparative performance of all models is described in Table 5.

Table 5. Comparative performance of models used

Model	Precision (landslide classes)	Recall (sensitivity)	Accuracy
CNN-1D (with early-stop)	89%	94%	91%
CNN-1D (100 epochs)	97%	94%	96%
Logistic regression	94%	98%	96%

4. CONCLUSION

The high scores of the proposed CNN-1D model show the superior predictive capability of applying deep learning neural networks on landslide susceptibility analysis with a score of 96% accuracy. The study also highlights a protocol using geospatial data directly. The geospatial data correspond to their real-world locations, which leads to a model with high predictive accuracy. In comparison, most of the study area is deemed to have very low susceptibility, much of the eastern portion where most landslide points are identified as very high susceptibility. On the western part of the Shikotsu Lake caldera, the surrounding areas are also deemed highly susceptible to landslides. Disaster mitigation programs and geotechnical engineering measures must be undertaken in landslide susceptible areas to lessen the potential socio-economic impact of future landslides. For future studies, further experiments using other convolutional layers (CNN-2D and CNN-3D) would be considered for a highly optimized predictive performance to create a hybrid deep neural network. Deep unsupervised neural networks such as autoencoders should also be used to observe the distribution patterns of potential landslide occurrences. Furthermore, using images instead of CSV files should be conducted to analyze inherent patterns of landslide features and maximize the potential of deep neural networks.

References:

Abdeljaber, O., Avci, O., Kiranyaz, S., Gabbouj, M., Inman, D.J. (2017). Real-time vibration-based structural damage detection using one-dimensional convolutional neural networks. Journal of Sound and Vibration, 388. 154-170. https://doi.org/10.1016/j.jsv.2016.10.043

Aimati, Y., Liu, W., Yamazaki, F., Maruyama, Y. (2019). Earthquake-induced landslide mapping for the 2018 Hokkaido Eastern Iburi earthquake using PALSAR-2 data. Remote Sensing, 11(20). https://doi.org/10.3390/rs11202351

Fang, Z., Wang, Y., Peng, L., Hong, H. (2020). Integration of convolutional neural network and conventional machine learning classifiers for landslide susceptibility mapping. Computers and Geosciences, 139(). https://doi.org/10.1016/j.cageo.2020.104470

Harbola, S., Coors, V. (2019). One dimensional convolutional neural network architectures for wind prediction. Energy Conversion and Management, 175. 70-75. https://doi.org/10.1016/j.enconman.2019.05.007

Liu, Y., Zhang, W., Zhang, Z., Xu, Q., Li, W. (2021). Risk factor detection and landslide susceptibility mapping using geo-detector and random forest models: The 2018 hokkaido eastern iburi earthquake. Remote Sensing, 13(6). https://doi.org/10.3390/rs13061157

Nam, K., Wang. F. (2019). The performance of using an autoencoder for prediction and susceptibility assessment of landslides: A case study on landslides triggered by the 2018 Hokkaido Eastern Iburi earthquake in Japan. Geoenvironmental Disasters, 6(1). https://doi.org/10.1186/s40677-019-0137-5

Nava, L., Monserrat, O., Catani, F. (2021) Improving Landslide Detection on SAR Data through Deep Learning. arXiv. http://arxiv.org/abs/2105.00782

Wang, Y., Fang, Z., Hong, H. (2019). Comparison of convolutional neural networks for landslide susceptibility mapping in Yanshan County, China. Science of the Total Environment, 666. 975-993. https://doi.org/10.1016/j.scitotenv.2019.02.263

Yimo, L., Zhang, W., Zhang, Z., Zhijie, X., Qiang, X., Weile, L. (2021). Risk factor detection and landslide susceptibility mapping using geo-detector and random forest models: The 2018 Hokkaido Eastern Iburi Earthquake. Remote Sensing, 13(6). https://doi.org/10.3390/rs13061157

Zhang, S., Li, R., Wang, F., Iio, A. (2019). Characteristics of landslides triggered by the 2018 Hokkaido Eastern Iburi earthquake, Northern Japan. Landslides, 16(9). 1691-1708. https://doi.org/10.1007/s10346-019-01207-6